Soil Biology and Biochemistry 196 (2024) 109505

Contents lists available at ScienceDirect

Soil Biology and Biochemistry

journal homepage: www.elsevier.com/locate/soilbio

Mechanisms behind high N_2O emissions from livestock enclosures in Kenya revealed by dual-isotope and functional gene analyses

Xiantao Fang [a,b,*], Stephen J. Harris [c], Sonja Maria Leitner [d], Klaus Butterbach-Bahl [d,e,f], Rafaela Feola Conz [a], Lutz Merbold [g], Michael Dannenmann [e], Antony Oyugi [d], Shuwei Liu [b], Jianwen Zou [b], Johan Six [a], Matti Barthel [a]

[a] Sustainable Agroecosystems Group, Department of Environmental Systems Science, ETH Zurich, Switzerland
[b] Key Laboratory of Low-carbon and Green Agriculture in Southeastern China, Ministry of Agriculture and Rural Affairs, College of Resources and Environmental Sciences, Nanjing Agricultural University, Nanjing, China
[c] School of Biological, Earth and Environmental Sciences, UNSW Sydney, NSW, Australia
[d] Mazingira Centre for Environmental Research and Education, International Livestock Research Institute (ILRI), Naivasha Rd, 00100, Nairobi, Kenya
[e] Karlsruhe Institute of Technology, Institute of Meteorology & Climate Research (IMK-IFU), Garmisch-Partenkirchen, Germany
[f] Pioneer Center Land-CRAFT, Agroecology, Aarhus University, Denmark
[g] Integrative Agroecology Group, Agroscope, Zurich, Switzerland

ARTICLE INFO

Keywords:
N_2O
Boma
Dual isotope mapping approach
Site preference
Functional genes

ABSTRACT

Livestock manure contributes to global warming due to greenhouse gas (GHG) emissions, especially nitrous oxide (N_2O) and methane (CH_4). In the arid and semi-arid lands of Sub-Saharan Africa (SSA), extensive pastoral grazing systems are common, with cattle grazing in the savanna during the day and kept in enclosures (called *bomas* in Kenya) during the night. Manure is usually not removed from bomas but left to accumulate, leading to excessive local nitrogen loads, making these bomas an overlooked N_2O emission hotspot in SSA that is currently not accounted for in national and regional GHG budgets. Here, we present the first *in-situ* isotope measurements of N_2O fluxes from 37 cattle bomas along an age gradient ranging from 0 to 5 years after boma abandonment in Kenya along with functional gene analysis of soil and manure samples. The isotopic composition of the emitted N_2O from bomas suggests that on average 91 ± 8% N_2O was produced via bacterial denitrification and/or nitrifier denitrification, with little variation across boma age class. We also found high levels of N_2O reduction to N_2 across all sample sites (81 ± 9%), indicating high levels of N_2O consumption. The abundances of denitrification-related genes (*nirK* and *narG*) were significantly higher than those of nitrification-related genes (*amoA*: AOA and AOB) in the cattle manure samples taken from the bomas, corroborating N_2O emissions largely being attributed to denitrification. Significant abundance of the reduction-related gene (*nosZ*) also corroborated the high potential for microbial N_2O reduction in bomas. Thus, by combining dual-isotope and functional gene analysis, we were able to identify source processes that govern N_2O emissions from these systems. More generally, making use of the manure by spreading it in the vicinity of the bomas or on dedicated forage plots could provide a win-win by enhancing savanna productivity while simultaneously mitigating GHG emissions.

1. Introduction

Nitrous oxide (N_2O) is an important contributor to global warming and stratospheric ozone depletion and thus plays a critical role in the global nitrogen (N) cycle (Ravishankara et al., 2009; Tian et al., 2020). Atmospheric N_2O concentrations have dramatically increased from pre-industrial levels of 270 ppbv–333 ppbv in 2020 (WMO, 2021) due to anthropogenic activities, especially livestock manure management and the use of synthetic and organic fertilizers to increase crop yields (Davidson, 2009; Tubiello et al., 2014; Tian et al., 2016). Over the past four decades, it is assumed that N_2O emissions from livestock manure increased significantly at a rate of 0.1 ± 0.01 Tg N yr^{-1} per decade (Tian et al., 2020).

The increase in N_2O emissions from terrestrial systems is closely linked to increased N availability for microbial nitrification and denitrification (Tian et al., 2016). During the last six decades, livestock

* Corresponding author. Sustainable Agroecosystems Group, Department of Environmental Systems Science, ETH Zurich, Switzerland.
E-mail address: 2020203024@stu.njau.edu.cn (X. Fang).

https://doi.org/10.1016/j.soilbio.2024.109505
Received 15 January 2024; Received in revised form 28 April 2024; Accepted 20 June 2024
Available online 21 June 2024

numbers on the African continent have increased dramatically to meet the growing demand of protein for a growing population (Butterbach--Bahl et al., 2020). Africa is home to 20% of the world's cattle, 27% of the sheep, and 31% of the goats, and most of these animals roam in the extensive grazing systems of Africa's arid and semi-arid lands (ASALs) (Gilbert et al., 2018). To protect them from theft and predators, livestock is usually kept in overnight enclosures ("bomas" in Kiswahili, "kraals" in Afrikaans, "corrals" in English). A single boma can be used from as short as one week up to years or even decades. Given the large quantities of manure that accumulate in bomas, they remain N_2O emission sources for years to decades after their abandonment (Butterbach-Bahl et al., 2020). Nevertheless, the processes of N transformation and N_2O formation and consumption during the use and after the abandonment of African cattle bomas have not been studied. Although some studies have focused on effects of bomas on soil nutrients and vegetation biodiversity (Marshall et al., 2018; Muchiru et al., 2008, 2009), there are only few studies that measured N_2O emissions in the field. A study conducted by Butterbach-Bahl et al. (2020) in Kenyan rangelands highlights significant N_2O emissions from bomas, which are often overlooked hotpots of N_2O emissions. Leitner et al. (2024) found that bomas contribute up to 32% of total N_2O emissions at farm-scale on a Kenyan cattle ranch. Zhu et al. (2024) found that sheep bomas are also large sources of N_2O emissions. However, the mechanisms underlying the high N_2O emissions from livestock enclosures remain unexplored.

In soils, the production of N_2O can be divided into biotic and abiotic processes (Baggs, 2008). Over the past decades, studies based on laboratory experiments have significantly advanced our understanding of the various biotic and abiotic mechanisms associated with the processes of N_2O formation from soils (Butterbach-Bahl et al., 2013). The biotic processes of nitrification and denitrification are considered to be the main pathways of N_2O production, contributing more than 70% to global N_2O emissions (Syakila and Kroeze, 2011; Tiedje, 1998). During nitrification, nitrite (NO_2^-) can be directly reduced to nitric oxide (NO) directly and followed by the reduction of NO to N_2O and N_2, resulting in nitrifier-denitrification (Kool et al., 2011; Wrage et al., 2001). If nitrifiers are considered responsible, the process is called nitrifier-denitrification, whereas it is called nitrification-coupled denitrification when denitrifiers are responsible. Moreover, dissimilatory nitrate reduction to ammonium (DNRA), which is performed by a diverse group of bacteria and fungi of the *Ascomycota* phylum, has also been found to be a relevant process for N_2O formation (Pandey et al., 2020; Silver et al., 2001; Tiedje, 1998). However, compared to laboratory incubation conditions with sieved soil, *in-situ* field conditions are different and more complex, causing challenges to study the production and consumption processes of N_2O (Wei et al., 2023). Quantifying the consumption of produced N_2O to N_2 is particularly challenging under field conditions (Friedl et al., 2020). The reasons for that are multifold, such as (i) the mixing of soil produced/consumed N_2O with background atmospheric N_2O in different soil layers and the subsequent diffusion to the atmosphere (Amundson et al., 2023), (ii) difficulties linking N_2O to a wide range of abiotic factors, (iii) competing of abiotic and biotic processes in soils under field conditions that makes distinguishing the different processes more difficult (Wei et al., 2023), and (iv) the complexity of N_2 gas diffusion processes in soils (Well et al., 2019).

New approaches of *in-situ* stable isotope techniques have become more widely available to explore the processes of N_2O emissions under field conditions (Harris et al., 2021; Su et al., 2022). In particular, the position-specific analysis of ^{15}N within the linear N_2O molecule (site preference; $\delta^{15}N^{SP}$) has gained attention over the past two decades because of its ability to distinguish between the production processes and consumption of N_2O (Decock and Six, 2013; Yu et al., 2020). While $\delta^{15}N^{bulk}$ describes the average $\delta^{15}N$ of the central ($\delta^{15}N^{\alpha}$) and terminal N atom ($\delta^{15}N^{\beta}$), $\delta^{15}N^{SP}$ is calculated as the difference between $\delta^{15}N^{\alpha}$ and $\delta^{15}N^{\beta}$. Unlike $\delta^{15}N^{bulk}$, $\delta^{15}N^{SP}$ is independent of the isotopic signature of the substrates, providing a more robust way to distinguish the different processes of N_2O production. One way to extract the information carried by the isotopic composition of N_2O is via the stable isotope mapping approach (Denk et al., 2017; Yu et al., 2020; Decock and Six, 2013; Toyoda et al., 2011; Lewicka-Szczebak et al., 2017; Wu et al., 2019). This method relies on the information carried by $\delta^{15}N^{bulk}$, $\delta^{15}N^{SP}$ and $\delta^{18}O$ of emitted N_2O to distinguish the different microbial production processes, as well as to further quantify the reduction of N_2O to N_2 during denitrification. So far, this method has been used in a wide range of terrestrial and aquatic systems, such as croplands (Li et al., 2021b; Gao et al., 2023; Wei et al., 2023; Verhoeven et al., 2019), forests (Gallarotti et al., 2021; Barthel et al., 2022), grasslands (Buchen et al., 2018; Ibraim et al., 2019), peatlands (Nishina et al., 2023; Berendt et al., 2023), lakes (Tischer et al., 2022; Liang et al., 2022), wastewater (Gruber et al., 2022), estuaries (Gao et al., 2020; Su et al., 2021; Ho et al., 2023) and oceanic waters (Breider et al., 2015).

Another way to improve our understanding of N_2O emissions is the analysis of microbial functional genes encoding for enzymes related to N_2O production and consumption processes (Hu et al., 2015). In general, nitrifiers can be analyzed by targeting nitrification-encoding genes (*amoA* for ammonia-oxidizing archaea [AOA] and bacteria [AOB]), and denitrifiers by targeting denitrification-encoding genes (*nirK, nirS* and *narG*) (Schauss et al., 2009; Kandeler et al., 2006). Moreover, the *nosZ* gene encodes the N_2O reductase that performs the last step in denitrification and can be used as a marker to determine the reduction of N_2O to N_2 (Henry et al., 2006; Sanford et al., 2012). Recently, the combination of both position-specific stable isotope analysis and functional genes has been used to overcome methodological weaknesses in the understanding of N_2O production and consumption processes in soils (Gallarotti et al., 2021; Guo et al., 2022; Wei et al., 2023), lakes (Liang et al., 2022), and sediments (Su et al., 2021) which was summarized lately in a review article (Deb et al., 2024).

Here, we combined analyses of the *in-situ* natural abundance N_2O dual-isotope signatures with microbial functional genes for nitrification and denitrification in cattle bomas to reveal the mechanisms behind high N_2O emissions from livestock enclosures in Kenya. We also assessed the potential of produced N_2O being further reduced to N_2 during denitrification, which adds to our understanding of N_2O production and consumption in livestock enclosures in Kenya. More specifically, we hypothesize that the overall boma N content decreases from time after abandonment due to continuous losses of gaseous N species and leaching. We further expect a general shift from a nitrification-dominated system to a denitrification-dominated system due to initial nitrification of ammonium from urea and the mineralization and subsequent nitrification of organic N. While these hypotheses are based on the change of substrate with time it is important to note that these processes are additionally driven by oxygen availability which changes over the course of the year due to changes in soil/manure moisture. If supported, these hypotheses would point towards a low bioavailable N retention in livestock systems and further confirm the large potential of livestock systems to contribute significantly to global N_2O emissions.

2. Materials and methods

2.1. Study areas

This study was conducted in October 2021 at the Kapiti Research Station and Wildlife Conservancy of the International Livestock Research Institute (ILRI; Carbonell et al., 2021) located in the semi-arid savanna region (1°35.8′W-1°40.9′W, 36°6.4′E-37°10.3′E) of the Athi-Kapiti ecosystem in Kenya. The Kapiti ranch is in Machakos County, southern Kenya, covering an area of 13,000 ha. The ranch is home to ca. 2500 cattle of the local Boran breed; 1200 sheep; and 250 Galla goats that coexist with wildlife such as lions, zebras, wildebeests, and giraffes. The soil in this area is classified as Vertisol (Leitner et al., 2024), and the climate is a tropical savanna climate with annual mean air temperature of 19.3 °C and annual mean precipitation of 550 mm (Zhu et al., 2024). The Kapiti ranch is divided into grazing units to

facilitate grassland management. Each grazing unit contains 3–4 herds of 100–150 cattle that graze in the grassland throughout the year, with minimal supplementation of minerals. Each herd is confined into a separate boma that measures 30 m diameter. Bomas are usually clustered in groups of 3–4 bomas, which are positioned at strategic locations to have daily access to water from water holes. Boma clusters are used for one to three months depending on rainfall history and pasture availability (Fig. S1a), after which clusters are abandoned and cattle are moved to a different grazing unit. In this study, a gradient of different boma ages from 0 to 5 years was selected for sampling. In addition, samples were taken from adjacent savanna sites (ca. 500 m from boma edge) for background measurements.

2.2. Nitrogen content and isotopic composition of manure and soil

In each boma cluster, a manure sample was taken from each individual boma (n = 3) by taking a handful of the entire manure layer without mineral soil, and subsequently combined to one composite sample per cluster. For soil sampling, the manure layer was carefully removed, and the top 5 cm mineral soil were sampled and also combined to one composite sample per cluster. Samples were dried at 50 °C, and C, N concentration, $\delta^{13}C$ and $\delta^{15}N$ natural abundance enrichment of soil and manure were measured with an elemental analyzer (Flash IRMS IsoLink CN, Thermo Scientific, Bremen Germany) coupled via a Conflo IV interface (Thermo Scientific GmbH, Bremen, Germany) to an isotope ratio mass spectrometer (Delta VPlus, Thermo Finnigan MAT GmbH, Bremen, Germany) (Arab et al., 2023) at the Center of Stable Isotope Analysis of KIT/IMK-IFU. Isotope values are given in delta notation referenced to AIR-N_2, V-PDB, and V-SMOW for ^{15}N, ^{13}C and ^{18}O respectively:

$$\delta^{Z}X = \left(\frac{R_{sample}}{R_{reference}} - 1\right)$$

where R refers to the ratio of $^{13}C/^{12}C$, $^{15}N/^{14}N$ or $^{18}O/^{16}O$ and ^{Z}X refers to the heavy stable isotope Z of the element X.

2.3. N_2O fluxes

N_2O flux measurements were conducted in each individual boma of an age cluster (n = 3) and at 3 adjacent savanna sites by using the fast-box chamber method (Fig. S1b). For this, a opaque static chamber with a diameter of 30 cm was coupled to an ultra-portable LGR-ICOS laser N_2O and CH_4 gas analyzer (ABB-Los Gatos Research Inc., Zurich, Switzerland) running at a measurement frequency of 1 Hz (Modell 909–0041) (Zhu et al., 2024). The chamber was permanently connected to the analyzer and repositioned at each site. The N_2O concentration change was measured for at least 5 min at each point and the individual flux rate was calculated by linear regression over the sample period with a running average of 1s interval. Additional samples were also taken for gas chromatography (GC) analysis to confirm LGR-ICOS readings. The comparison between the LGR and GC showed a good agreement (R^2 = 0.93) between them, but the GC tended to measure slightly higher concentrations than the LGR (slope = 1.16). Note, it was often difficult to perfectly match the manual sampling with the LGR readings as concentrations were increasing very rapidly during manual sample withdrawal which in part explains the slight mismatch.

N_2O fluxes were measured at 37 individual bomas during the dry season. Due to the dry conditions, N_2O fluxes were too low to analytically measure the position-specific isotopic composition of N_2O (Wei et al., 2023). In order to stimulate N_2O flux rates to obtain more robust N_2O isotope measurements, 30 of the 37 measurement sites were rewetted with a simulated 20 mm rain event prior to N_2O flux measurement. Sampling took place approximately 10 min after rewetting.

2.4. N_2O position-specific isotope analysis

Position-specific N_2O isotope analysis ($\delta^{15}N^{bulk}$, $\delta^{18}O$, $\delta^{15}N^{SP}$) was conducted using the mixing model approach as described in Krüger et al. (2001). That is, during the placing of the chamber and immediately before chamber removal, gas samples for the analysis of the N_2O isotopic composition were withdrawn from the chamber headspace using a 60 mL syringe (Fig. S1). For each sample, a total amount of 180 mL of gas were stored in 110 mL serum crimp vials and shipped to ETH Zurich for analysis. $\delta^{15}N^{bulk}$, $\delta^{18}O$, and $\delta^{15}N^{SP}$ of emitted N_2O were measured using a gas preparation unit (Trace Gas, Elementar, MCR, UK) coupled to an IRMS (IsoPrime100, Elementar, MCR, UK) at ETH Zurich. For a detailed description of the measurement system and calibration refer to Verhoeven et al. (2019) and Gallarotti et al. (2021). The isotopic signature of the emitted N_2O ($[\delta^{Z}X$) was then calculated using:

$$\delta^{Z}X = \frac{[N_2O]_e \times [\delta^{Z}X]_e - [N_2O]_s \times [\delta^{Z}X]_s}{[N_2O]_e - [N_2O]_s}$$

where $[N_2O]_s$ and $[N_2O]_e$ are the N_2O mixing ratios [ppmv] in the samples at the start and at the end, respectively, and $[\delta^{Z}X]_s$ and $[\delta^{Z}X\ ]_e$ are the corresponding δ-values [‰] of the N_2O samples. Respective N_2O concentrations of LGR were recorded during sampling for N_2O isotopes.

2.5. N_2O isotope mapping approach

To determine the main production pathways of N_2O and quantify the reduction percentage of N_2O to N_2, we applied a dual isotopic mapping approach as described in Lewicka-Szczebak et al. (2017). We produced two dual isotope maps of SP-N_2O/$\delta^{15}N^{bulk}$-N_2O signatures and SP-N_2O/$\delta^{18}O$-N_2O signatures with the expected range of end-member isotopic signatures for nitrification, bacterial denitrification, nitrifier denitrification and fungal denitrification. In short, two scenarios were considered to quantify the shift in isotopic compositions of our samples: (1) a reduction then mixing scenario in which N_2O sourced from denitrification is first reduced, leaving a fraction of unreduced N_2O, which is then mixed with N_2O sourced from nitrification; and (2) a mixing then reduction scenario in which N_2O sourced from denitrification is first mixed with N_2O sourced from nitrification and then reduced to N_2 (Lewicka-Szczebak et al., 2017). The fraction of N_2O derived by denitrification (in this case bacterial denitrification and/or nitrifier denitrification) and the amount of reduced N_2O was then semi-quantitatively estimated for every sample using N_2O reduction slopes and mixing trajectories between possible end-member N_2O production pathways (Wu et al., 2019). We interpret and discuss semi-quantitative estimates from the reduction then mixing scenario given that it has been argued to be the most likely process leading to observed isotope signatures from N_2O emitted from soils (Wu et al., 2019). Due to the large range in end-member ranges in the SP-N_2O/$\delta^{15}N^{bulk}$-N_2O mapping approach, we discuss here only estimates from the SP-N_2O/$\delta^{18}O$–N_2O isotope maps.

In the isotope mapping approach, the fraction of N_2O derived by bacterial denitrification and/or nitrifier denitrification (often collectively termed denitrification) and the fraction of reduced N_2O can be semi-quantitatively estimated for every sample using N_2O reduction slopes and mixing trajectories between possible end-member N_2O production pathways (Lewicka-Szczebak et al., 2017; Wu et al., 2019; Yu et al., 2020). In this study, reduction slopes were taken from Yu et al. (2020) and ranged from 0.23 to 0.98 with a mean of 0.45 for $\delta^{15}_{N2\text{-}N2O}N^{SP}/\delta^{18}_{N2\text{-}N2O}O$ and from 0.51 to 2.78 with a mean of 0.96 for $\delta^{15}_{N2\text{-}N2O}N^{SP}/\delta^{15}_{N2\text{-}N2O}N^{Bulk}$. Respective end-member $\delta^{15}N$ values, $\delta^{18}O$ and SP values were also derived from Yu et al. (2020). We corrected our isotope source fields for bacterial denitrification, nitrifier denitrification and fungal denitrification using average $\delta^{18}O$-H_2O values in precipitation ($\delta^{18}O = -3.34‰$, n = 15) taken at the nearest location to our study area (Muguga; latitude: −1.22, longitude: 36.63) accessed via the GNIP database. Because of the stable nature of atmospheric $\delta^{18}O$–O_2 and the

absence of direct measurement, $\delta^{18}O$ end-member values for nitrification were not corrected for substrate composition. Note that we assumed a value of 0‰ for $\delta^{15}N$ in the precursor nitrate and ammonia in our SP-N_2O/$\delta^{15}N^{bulk}$-N_2O map. We used mean values for mixing, fractionation, and reduction whenever possible. However, if samples were distributed outside the mean mixing-reduction area, we used either their minimum or maximum values, in keeping with previous studies using this methodology (e.g., Buchen et al., 2018).

In addition to the dual isotope mapping approach, we analyzed our data using a newly developed tool based on the Markov-Chain Monte Carlo (MCMC) algorithm known as Fractionation And Mixing Evaluation (FRAME; Lewicki et al., 2022). This was undertaken to ensure our dual isotope mapping results produced reasonably similar results had we modelled three-dimensional mixing and reduction using $\delta^{15}N^{bulk}$-N_2O in addition to SP-N_2O and $\delta^{18}O$-N_2O. A comparison between these two approaches can be found in the Supporting Information. Our results have also been qualitatively compared and validated against mixing and reduction estimates acquired using TimeFRAME (Harris et al., 2023).

2.6. Gene abundance

We performed Real-time qPCR to measure each abundance of nitrification-related and denitrification-related microbial group including ammonia monooxygenase (*amoA*: AOA and AOB), nitrate reductase (*narG*), nitrite reductase (*nirK*), and nitrous oxide reductase (*nosZ*). DNA from the collected soil and manure samples were extracted from 0.25 g fresh soil or manure using the DNeasy Pro PowerSoil Kit (Qiagen, Hilden, Germany) according to the manufacturer's recommendation using the QIAcube System (Qiagen). Using the QIAxpert System (Qiagen, Hilden, Germany), we measured the concentration of DNA through UV/Vis spectrophotometry. To reduce inhibition, the extracted DNA was diluted to 10 ng/L. Employing a SYBR Green-based qPCR approach, we evaluated the abundance of functional groups. We tested the presence of inhibitory compounds that may have been co-extracted during DNA extraction by introducing pGEM-T plasmid (GenBank® Accession No. X65308; Promega, Madison, WI, United States) into all samples at equimolar concentrations and amplifying a region on the plasmid using specific primers SP6 and T7 (Microsynth). The qPCR standards were produced using purified PCR products of each functional gene obtained by pooling normalized DNA from all samples, and subsequently were diluted to obtain a standard curve comprising of the concentrations ranging from 10^{-7} to 10^{-3} ng of the target template. A negative control containing PCR grade water was included. The information about the primers used for each functional genes including primers name, sequence, thermal profile and produced size is detailed in Table S1. Each reaction was conducted with 0.4 μM of each primer, 1X SSO AdvancedTM Universal SYBR Green Supermix (Bio-Rad Laboratories, Hercules, CA, United States), and 40 ng of template DNA. The cycling conditions for all reactions included a polymerase activation step at 98 °C for 3 min, denaturation at 95 °C for 15s, annealing at primer-specific temperatures (see Table S1) for 30 s, elongation at 72 °C for 15s, followed by image acquisition at 80 °C for 15s. All qPCRs were performed in technical triplicates using a thermocycler CFX96 Touch Real-Time System (Bio-Rad Laboratories, Hercules, CA, United States). To verify the amplification specificity, melting curves were generated. The results were documented and analyzed using the CFX Maestro software (Bio-Rad Laboratories, Hercules, CA, United States). For all runs, the qPCR efficiency was 80-95%, and the R^2 value was >0.99.

2.7. Data analysis

Differences between N content and $\delta^{15}N$ values in soil and manure, as well as differences between abundance of functional genes in bomas with different years since boma abandonment and savanna sites were evaluated using one way and two-way analyses of variance (ANOVA) with Tukey's HSD test. Testing for normality distribution and variance heterogeneity was done using the Shapiro-Wilk test and Levene's test. The correlations between $\delta^{15}N$ value in soil/manure and boma age were examined by spearman correlation analyses. All statistical analyses were performed using R, all plots were generated using R (Version 4.1.3), and statistical significance was determined at the 0.05 probability level.

3. Results

3.1. Physicochemical soil characteristics

Soil N content in bomas averaged 0.25 ± 0.02%, which was significantly higher than in adjacent savanna soil (0.05%) ($p < 0.01$, Fig. 1a). The N content in manure of bomas averaged 1.50 ± 0.08%, which was significantly higher than that in soil of bomas ($p < 0.01$, Fig. 1a). N content of boma soils or manure did not change with boma age. However, soil $\delta^{15}N$ values in bomas showed a significant increase with age since boma abandonment (from 6.83 to 10.59‰) and were significantly higher in all age classes than in background savanna soil (5.61‰) ($p < 0.01$, Fig. 1b). Moreover, the averaged $\delta^{15}N$ value in boma manure was lower than that in boma soil, and also increased with boma age (from 2.77 to 10.60‰) (Fig. 1b). The C/N ratio in manure was significantly higher than that in boma soil, and it showed a significantly decrease with age since boma abandonment in both manure and soil of boma ($p < 0.01$, Fig. 1c). However, the C/N ratio in boma soil was significantly lower than that in background savanna soil ($p < 0.01$, Fig. 1c). The $\delta^{13}C$ in boma soil was significantly higher than that in manure (Fig. S3).

3.2. N_2O fluxes and isotopic signatures

N_2O fluxes in bomas (n = 37) averaged 2983 ± 561 μg N m^{-2} h^{-1} with a range of 21–15698 μg N m^{-2} h^{-1}, which was significantly higher than that in savanna soil (4.79 ± 0.43 μg N m^{-2} h^{-1}, n = 3) ($p < 0.01$, Fig. S2). N_2O fluxes did not differ between different boma age classes (Fig. S2). Overall, observed $\delta^{15}N^{bulk}$-N_2O values in all bomas remained relatively low (mean: −9.54 ± 0.93‰), and ranged from −21.91‰ to 0.78‰ (Fig. 2a). The observed $\delta^{18}O$-N_2O values in all bomas ranged from 27.02 to 69.78‰ (mean: 43.43 ± 1.52‰) (Fig. 2b). The measured $\delta^{15}N^{SP}$-N_2O values in all bomas averaged 1.36 ± 0.62‰, which ranged from −3.93 to 11.63‰ (Fig. 2a).

3.3. Isotopic mapping and modelling

Plots of $\delta^{15}N^{bulk}$-N_2O and $\delta^{15}N^{SP}$-N_2O showed that 80% of our data clustered in the area of heterotrophic bacterial denitrification (Fig. 2a), and plots of $\delta^{18}O$-N_2O and $\delta^{15}N^{SP}$-N_2O showed the distribution of data was broadly consistent with the theoretical N_2O reduction line (Fig. 2b). Using our $\delta^{18}O$-N_2O/$\delta^{15}N^{SP}$-N_2O mapping approach, we estimated that residual N_2O fractions (rN_2O; the fraction of residual N_2O remaining after reduction to N_2) averaged 19 ± 9% (mean ± 1s.d.), corresponding to an average 81 ± 9% reduction of N_2O to N_2 (Fig. 4a). Among different ages since boma abandonment, the reduction from N_2O to N_2 within the 5 years after boma abandonment ranged from 60 to 98% (Fig. 4a). However, the reduction percent showed no significant difference between boma ages, meaning the reduction from N_2O to N_2 remained at a steady level after boma abandonment (Fig. 4a). Similarly, we estimated that bacterial denitrification and/or nitrifier denitrification contributed on average 91 ± 8% to N_2O production, and nitrification and/or fungal denitrification contributed on average 9 ± 8% to N_2O production (Fig. 4b).

3.4. Gene abundance

We measured abundance of functional genes related to nitrification and denitrification. Typically, the mean abundance of denitrification-related functional genes (*nirK*, *narG*) was significantly higher than that of nitrification-related functional genes (AOA *amoA* and AOB *amoA*) (p

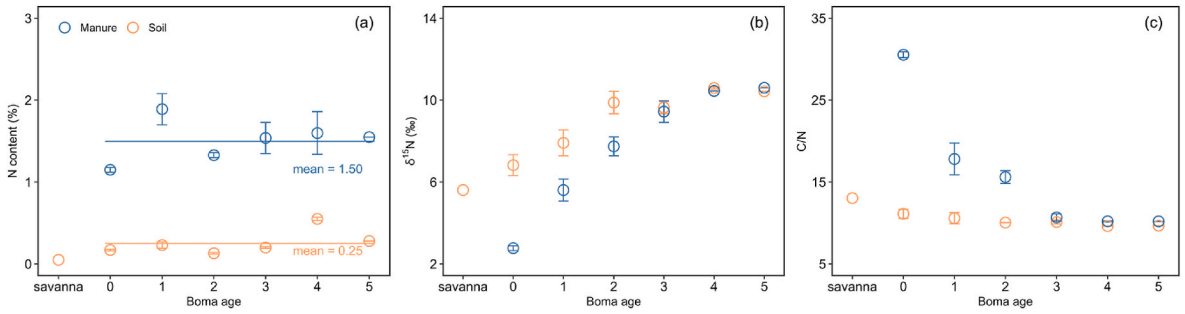

Fig. 1. Change of (a) N content (%), (b) $\delta^{15}N$ value (‰) and (c) C/N ratio in soil and manure of cattle bomas with different years since boma abandonment; background savanna site is given as a reference. The orange and blue lines in (a) show the mean N content in soil and manure of bomas.

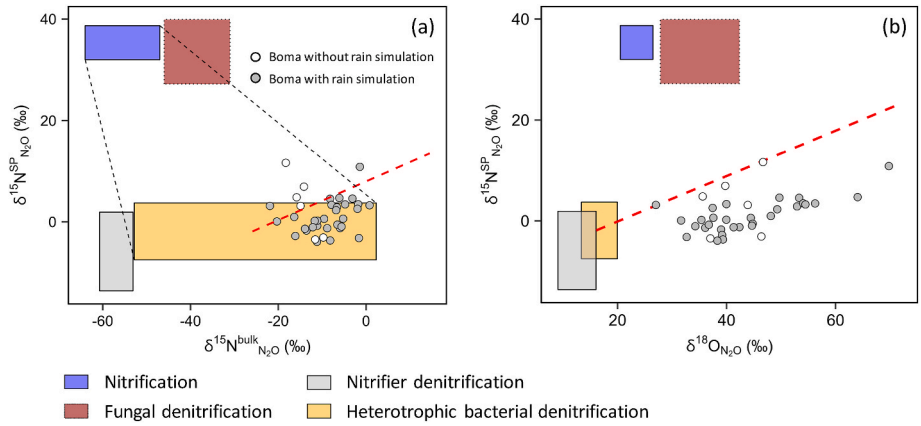

Fig. 2. Dual isotope maps for $\delta^{15}N^{bulk}$, $\delta^{15}N^{SP}$ and $\delta^{18}O$; (a) $\delta^{15}N^{SP}$ vs. $\delta^{15}N^{bulk}$ dual isotope map and (b) $\delta^{15}N^{SP}$ vs. $\delta^{18}O$ dual isotope map. The red dashed lines show the theoretical reduction line from N_2O to N_2. The area in between the black dashed lines in (a) show the area of mixing between nitrification and denitrification. End-member values of the different boxes and slopes of reduction lines are based on Yu et al., (2020). Note that in (a), source fields are plotted assuming the substrate $\delta^{15}N$ signature is 0 ‰.

< 0.01; Fig. 3a and b). The abundance of AOB in bomas increased with increasing years after boma abandonment (Fig. 3a). The mean abundance of AOB in boma soil was significantly higher than in savanna soil (7.77×10^2) (Fig. 3a). The abundance of AOA in boma soil also increased with increasing years after boma abandonment, while it showed lower level of abundance than AOB (Fig. 3a). However, differing from AOB, the abundance of AOA was higher in savanna soil (1.92×10^4) than in bomas.

Copy numbers of *nirK* and *narG* in boma manure were significantly higher than in savanna soil (*nirK*: 3.03×10^5 and *narG*: 4.24×10^4) ($p < 0.01$, Fig. 3b). Moreover, the copy number of *nirK* and *narG* increased in the first year since boma abandonment, and then remained constant during the following years (Fig. 3b). Copy numbers of *nirk* and *narG* during the 1-5 years since boma abandonment were stable around $1.74 \times 10^6 \pm 6.43 \times 10^4$ and $5.26 \times 10^5 \pm 4.27 \times 10^4$, respectively (Fig. 3b). Similarly, copy numbers of *nosZ* in boma soil increased in the first year since boma abandonment and then remained at a steady level (1.44×10^5), and it was also significantly higher than in savanna soil (1.05×10^4) ($p < 0.01$, Fig. 3c).

4. Discussion

4.1. N_2O production in bomas

Livestock enclosed in bomas at night produce abundant manure, which greatly enriches soil microbial N availability in bomas.

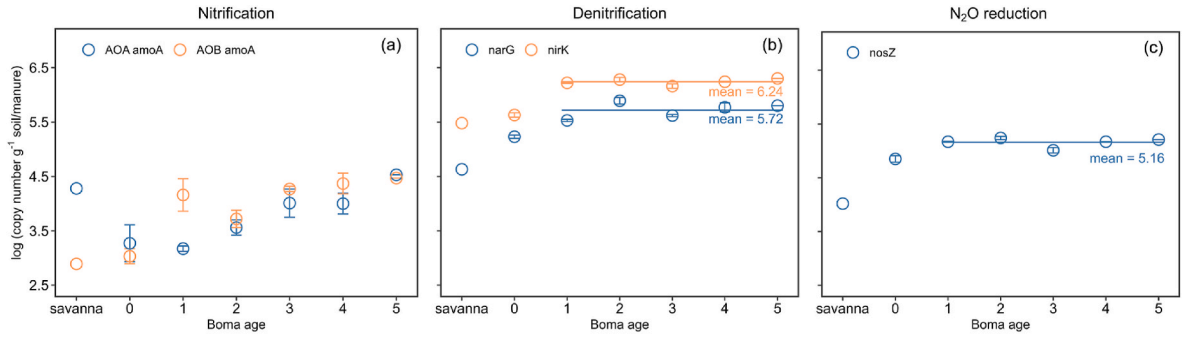

Fig. 3. Change of the abundance of functional genes of N_2O production and consumption processes in the manure layer of cattle bomas along an age gradient; background savanna site is given as a reference. (a) Nitrification (AOA *amoA* and AOB *amoA* genes), (b) denitrification (*narG* and *nirK* genes) and (c) N_2O reduction (*nosZ* gene). The orange and blue lines show the mean abundance of functional genes of bomas from 1 to 5 years since boma abandonment.

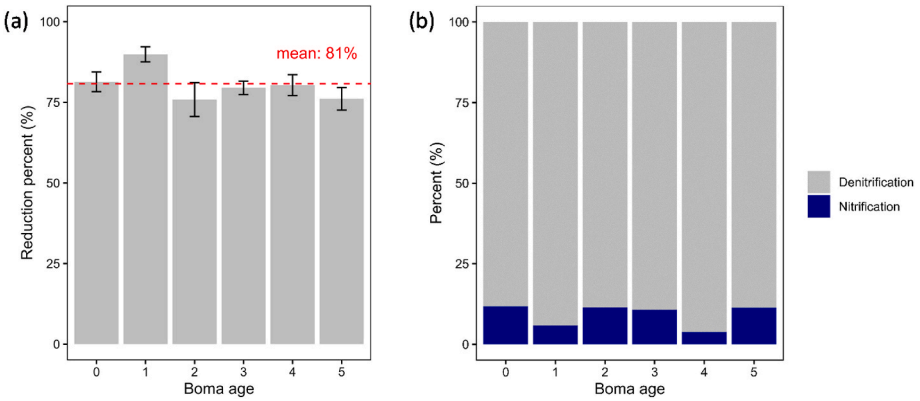

Fig. 4. Change in (a) reduction percent (%) of N_2O to N_2 and (b) percent (%) of nitrification and denitrification calculated based on the N_2O isotope mapping approach along the boma age gradient (0–5 years). The red dotted lines in (a) shows the mean reduction percent across all cattle bomas. Note, in (b), denitrification refers to bacterial denitrification and nitrifier denitrification, while nitrification refers to nitrification and fungal denitrification.

Consequently, manure also caused the soil N content below the manure layer to increase in our study, most likely due to N leaching, from 0.05% total N in savanna soil to an average of 0.25% total N in soils across all boma age classes. In contrast to our expectations, N content in soil and manure across age classes did not decrease with time but was rather stable. This is in line with the findings of Butterbach-Bahl et al. (2020) who found sustained N_2O fluxes even 40 years after boma abandonment. Our result of $\delta^{15}N$ in manure is in the range (2.6–21.3‰) reported by Bedard-Haughn et al. (2003). It is important to note, that the numbers of Bedard-Haughn et al. (2003) are mainly based on cattle fed with soybean while savanna cattle primarily forage on savanna grassland vegetation with high lignin content. While the N content was stable over time in both manure and boma soil (Fig. 1a), the $\delta^{15}N$ value increased steadily during the first 3 years after boma abandonment before levelling out (Fig. 1b). The increasing $\delta^{15}N$ signature in both soil and manure points to a strong continuous N loss (gaseous and/or leaching) especially during the first 3 years after boma abandonment. Initially, $\delta^{15}N$ of manure and boma soil below showed a difference of about 4‰, but it converged after 3 years of boma abandonment. The reasons for this difference can be manifold, such as forage, N deposition (Carbonell et al., 2021), NH_3 volatilization, gaseous N loss, and/or N leaching. The initial 4‰ depletion of ^{15}N in manure (as compared to soil) can be explained by the only partly digested plant material which composes most of the manure material. This is corroborated by the higher C/N ratio of manure especially in the early phase after abandonment. If we look at the relative enrichment ($\delta^{15}N_{manure}$ - $\delta^{15}N_{soil}$; Fig. S4), we observe an enrichment of manure relative to soil during the first two years, probably due to gaseous as well as leaching N losses. As the boma ages, both, the C/N ratio and $\delta^{15}N$ signature of soil and manure converge as the manure and soil becoming more mixed.

The manure-derived excess N in bomas likely caused N_2O emissions to soar compared to the savanna background with flux rates similar to those observed by previous studies (Butterbach-Bahl et al., 2020; Zhu et al., 2024). Our analysis of the isotopic composition of N_2O revealed

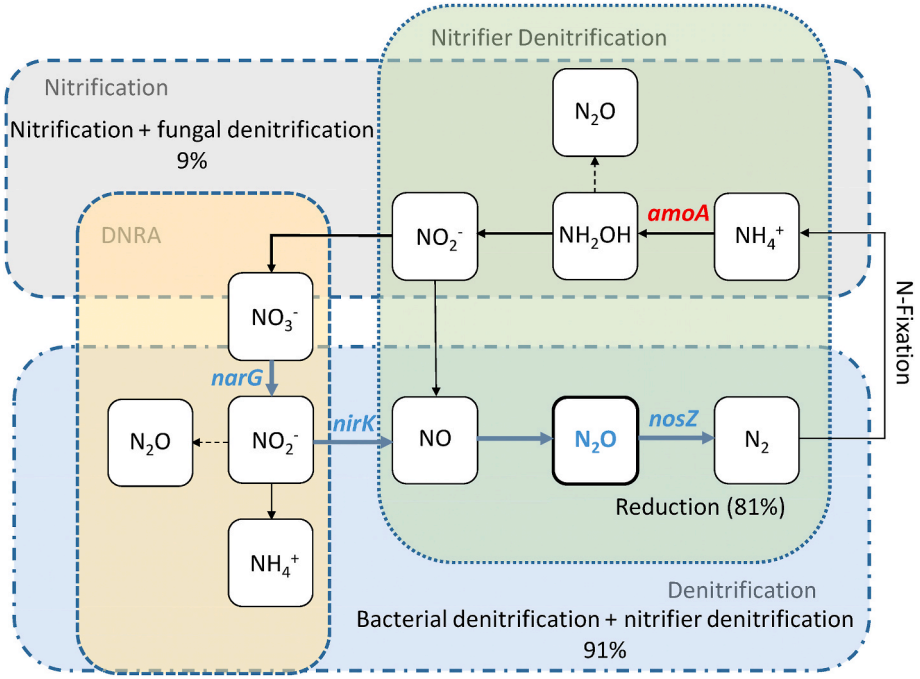

Fig. 5. Main biotic N_2O production and consumption pathways (nitrification, denitrification, nitrifier-denitrification, and dissimilatory nitrate reduction to ammonium DNRA) in cattle bomas. The thick lines show the main process of N_2O production and consumption in cattle bomas. The percentage of nitrification + fungal denitrification (9%) and bacterial denitrification + nitrifier denitrification (91%), and the reduction percent (81%) are estimated based on the modelling approach detailed in the methods section. This figure is modified after Gallarotti et al. (2021).

that heterotrophic bacterial denitrification dominated N_2O emissions of bomas in Kapiti (Fig. 2a). The isotope mapping of $\delta^{15}N^{bulk}$-N_2O and $\delta^{15}N^{SP}$-N_2O shows that most data (80%) clustered in the area assigned to heterotrophic bacterial denitrification (Fig. 3a). This qualitative assessment is in line with several other *in-situ* studies, which found a high contribution of heterotrophic bacterial denitrification to total denitrification in forests and croplands (e.g. Gallarotti et al., 2021; Wei et al., 2023). Our $\delta^{15}N^{SP}$-N_2O/$\delta^{18}O$-N_2O model results showed that 91 ± 8% of produced N_2O originated from heterotrophic bacterial denitrification and/or nitrifier denitrification), while only 9 ± 8% was produced from nitrification and/or fungal denitrification (Figs. 4b and 5). Our results are in line with other *in-situ* studies from farming systems which also found that denitrification dominated total N_2O emission in grasslands (Wolf et al., 2015; Ibraim et al., 2019, 2020; Harris et al., 2021) and croplands (Wei et al., 2023; Gao et al., 2023). We note, however, that a rewetting pulse as conducted in our study might stimulate substantial N_2O emissions due to strong microbial respiration which in turn causes a rapid depletion in soil oxygen, creating anaerobic microsites which favor denitrification (Hu et al., 2017; Leitner et al., 2017). Rewetting of dried soil and manure is a common scenario in the semi-arid rangelands where this study took place. The research site has two wet seasons (Apr.–Jun. and Oct.–Dec.) and also experiences irregular rain events during dry seasons. In a previous study from the same study site that was recently published (Leitner et al., 2024), N_2O from cattle bomas was measured over a full year and several rewetting N_2O pulses were observed. In fact, rain was the main driver of N_2O emissions from abandoned bomas that were not actively used. This seems logical because the manure layer dries out quickly under the hot savanna climate, thereby reducing N_2O emissions due to water limitation. Once it rains, microbial activity increases, driving N transformation and promoting N_2O emissions. Similar patterns of low N_2O emissions under dry conditions and pulsed N_2O emissions during rainy periods have been observed by others as well, who have found that rainfall seasonality is the main driver of GHG emissions and soil processes in semi-arid savannas (particularly after manure deposition), whereas temperature plays only a minor role because there is little variation (Scholes et al., 1997; Pelster et al., 2016; Wachiye et al., 2020; Zhu et al., 2024). Alternatively, the measured isotopic signature might reflect the N_2O which had accumulated in pores and is released upon filling the pores with water. However, we observed similar results from the isotopic mapping for the non-rewetted bomas which points to the fact that denitrification occurs independently of moisture status.

Given the above-mentioned challenges to accurately interpret N_2O isotopic mapping results using a rewetting pulse to stimulate emissions, we further explored the functional genes related to the N cycle to verify our isotope results. The abundances of N-cycling functional genes are recognized as a strong indicator for linking the microbial community to N_2O emissions (Baggs, 2008; Butterbach-Bahl et al., 2013). Our results of functional genes showed a significantly higher abundance of denitrification-related genes than nitrification-related genes (Fig. 3), which also supports that denitrification is the main process underlying the N_2O emissions in bomas. Nevertheless, it has been shown that denitrifier gene abundance is not always directly linked to N_2O emissions, but rather gene expression (RNA level or even protein level) being a better predictor for N_2O emissions (Zhang et al., 2022; Wang et al., 2018).

4.2. N_2O consumption in bomas

The emission of N_2O is not only controlled by N_2O production but also the consumption of produced N_2O through total denitrification (Butterbach-Bahl et al., 2013). The reduction of N_2O to N_2, facilitated by the enzyme N_2O reductase, is probably the most important biological process for the consumption of N_2O (Li et al., 2021a). We have demonstrated that denitrification was the main process of N_2O emission in bomas and also quantified the extent of total denitrification through isotopic mapping. Our isotope modelling showed that the averaged reduction percent of N_2O to N_2 was 81 ± 9% (Fig. 4a), which was substantially higher compared to observations from other grassland soils (30–70%) (Ibraim et al., 2020), croplands (52–64%) (Li et al., 2021b), or peatlands (9–48%) (Berendt et al., 2023). High reduction of produced N_2O to N_2 in bomas could be caused by the elevated soil/manure bulk density in bomas due to trampling of livestock in the confined area over extended periods of time; the high bulk density reduces diffusion of N_2O out of the soil/manure matrix and oxygen into the soil/manure pore space, which stimulates total denitrification and thus N_2O reduction to N_2 (Kuang et al., 2019). It is, the reduction of produced N_2O to N_2 during upward diffusion is mainly correlated to the residence time and the length of the diffusion pathway of N_2O in the soil/manure matrix (Castle et al., 1998; Goldberg et al., 2008).

In addition to the isotopic mapping results of reduction, the functional gene analysis also showed a high enzymatic potential of N_2O reduction in bomas (total denitrification), indicated by a high gene copy number of the *nosZ* gene relative to the nitrifying genes. Thus, both the isotopes and the functional genes indicate that total denitrification is a dominant process in bomas (Fig. 5).

4.3. Implications for boma management

Bomas are substantial N_2O emission sources at the landscape scale, and the current practice is that manure is usually not removed but left to decompose in the bomas. In order to mitigate N_2O emissions from pastoral areas, livestock keepers could consider using boma manure as fertilizer on the adjacent grassland, thereby replacing N removed through biomass consumption by grazing livestock. They could further apply boma manure on dedicated forage plots to produce feed for periods of scarcity such as the dry season or extended drought periods. These practices would not only reduce N_2O emissions from bomas, but have the potential to increase rangeland productivity and resilience.

5. Conclusion

Our study explored the mechanisms behind N_2O emissions from livestock enclosures in Kenya. By combining *in-situ* dual isotope and functional gene analysis, we gained insights into the processes of N_2O production and consumption in bomas. Both methods suggest that denitrification processes dominated N_2O emissions from bomas. Moreover, both methods further agreed that a substantial proportion of produced N_2O undergoes further reduction to N_2. We believe that the combination of several methods is key to unravel the complex mechanisms of N_2O production/consumption as both have their individual limitation such as extraction efficiencies (functional genes) or detection limits (dual isotope mapping). Overall, our results provide first insights into underlying mechanisms of N_2O production and consumption in bomas and provide a basis to quantify livestock related fluxes from N_2O emissions hotspots in Sub-Saharan Africa as a basis for targeting interventions to mitigate emissions.

CRediT authorship contribution statement

Xiantao Fang: Writing – review & editing, Writing – original draft, Software, Formal analysis. **Stephen J. Harris:** Software, Methodology. **Sonja Maria Leitner:** Writing – review & editing. **Klaus Butterbach-Bahl:** Writing – review & editing, Data curation. **Rafaela Feola Conz:** Methodology, Data curation. **Lutz Merbold:** Writing – review & editing, Data curation. **Michael Dannenmann:** Writing – review & editing. **Antony Oyugi:** Data curation. **Shuwei Liu:** Writing – review & editing. **Jianwen Zou:** Writing – review & editing. **Johan Six:** Writing – review & editing, Supervision, Project administration, Funding acquisition. **Matti Barthel:** Writing – review & editing, Supervision, Project administration, Methodology, Investigation, Data curation.

Declaration of competing interest

The authors declare that they have no known competing financial interests or personal relationships that could have appeared to influence the work reported in this paper.

Data availability

Data will be made available on request.

Acknowledgements

We like to thank our assistants Elly Kibira and Nelson Kipchirchir at Kapiti Ranch for knowledge on boma ages and general assistance in the field. This work was supported by ETH Core funding to JS and MB. KBB received funding from the Pioneer Center for Research in Sustainable Agricultural Futures (Land-CRAFT), DNRF grant number P2. LM acknowledges funding received from the European Union's Horizon Europe Programme (grant agreement number 101058525) for the project "Knowledge and climate services from an African observation and Data research Infrastructure (KADI)". SL acknowledges additional financial support of the CGIAR Research Initiatives Livestock and Climate and Mitigate+: Low-Emission Food Systems, which are supported by contributors to the CGIAR Trust Fund. Furthermore, SL was supported through the EU-DeSIRA "ESSA" project (Earth observation and environmental sensing for climate-smart sustainable agro-pastoral ecosystem transformation in East Africa). This work was supported by the National Key Research and Development Program of China (2022YFD1901600) and the Guidance Foundation, the Sanya Institute of Nanjing Agricultural University (KYTZ2023017). Xiantao Fang was supported by China Scholarship Council (No. 202206850036).

Appendix A. Supplementary data

Supplementary data to this article can be found online at https://doi.org/10.1016/j.soilbio.2024.109505.

References

Amundson, R., Mills, J.V., Lammers, L.N., Barthel, M., Gallarotti, N., Six, J., Gebauer, G., Maurer, G.E., 2023. Simultaneous production and consumption of soil N_2O creates complex effects on its stable isotope composition. Global Biogeochemical Cycles 37, e2022GB007536.

Arab, L., Hoshika, Y., Paoletti, E., White, P.J., Dannenmann, M., Mueller, H., Ache, P., Hedrich, R., Alfarraj, S., Albasher, G., Rennenberg, H., 2023. Chronic ozone exposure impairs the mineral nutrition of date palm (Phoenix dactylifera) seedlings. Science of the Total Environment 862, 160675.

Baggs, E.M., 2008. A review of stable isotope techniques for N_2O source partitioning in soils: recent progress, remaining challenges and future considerations. Rapid Communications in Mass Spectrometry 22, 1664–1672.

Barthel, M., Bauters, M., Baumgartner, S., Drake, T.W., Bey, N.M., Bush, G., Boeckx, P., Botefa, C.I., Deriaz, N., Ekamba, G.L., Gallarotti, N., Mbayu, F.M., Mugula, J.K., Makelele, I.A., Mbongo, C.E., Mohn, J., Mandea, J.Z., Mpambi, D.M., Ntaboba, L.C., Rukeza, M.B., Spencer, R.G.M., Summerauer, L., Vanlauwe, B., Van Oost, K., Wolf, B., Six, J., 2022. Low N_2O and variable CH_4 fluxes from tropical forest soils of the Congo Basin. Nature Communications 13, 330.

Bedard-Haughn, A., Van Groenigen, J.W., Van Kessel, C., 2003. Tracing ^{15}N through landscapes: potential uses and precautions. Journal of Hydrology 272, 175–190.

Berendt, J., Jurasinski, G., Wrage-Monnig, N., 2023. Influence of rewetting on N_2O emissions in three different fen types. Nutrient Cycling in Agroecosystems 125, 277–293.

Breider, F., Yoshikawa, C., Abe, H., Toyoda, S., Yoshida, N., 2015. Origin and fluxes of nitrous oxide along a latitudinal transect in western North Pacific: controls and regional significance. Global Biogeochemical Cycles 29, 1014–1027.

Buchen, C., Lewicka-Szczebak, D., Flessa, H., Well, R., 2018. Estimating N_2O processes during grassland renewal and grassland conversion to maize cropping using N_2O isotopocules. Rapid Communications in Mass Spectrometry 32, 1053–1067.

Butterbach-Bahl, K., Baggs, E.M., Dannenmann, M., Kiese, R., Zechmeister-Boltenstern, S., 2013. Nitrous Oxide Emissions from Soils: How Well Do We Understand the Processes and Their Controls?, 368. Philosophical Transactions of the Royal Society B-Biological Sciences, 20130122.

Butterbach-Bahl, K., Gettel, G., Kiese, R., Fuchs, K., Werner, C., Rahimi, J., Barthel, M., Merbold, L., 2020. Livestock enclosures in drylands of Sub-Saharan Africa are overlooked hotspots of N_2O emissions. Nature Communications 11, 4644.

Carbonell, V., Merbold, L., Díaz-Pinés, E., Dowling, T.P.F., Butterbach-Bahl, K., 2021. Nitrogen cycling in pastoral livestock systems in Sub-Saharan Africa: knowns and unknowns. Ecological Applications 31.

Castle, K., Arah, J.R.M., Vinten, A.J.A., 1998. Denitrification in intact subsoil cores. Biology and Fertility of Soils 28, 12–18.

Davidson, E.A., 2009. The contribution of manure and fertilizer nitrogen to atmospheric nitrous oxide since 1860. Nature Geoscience 2, 659–662.

Deb, S., Lewicka-Szczebak, D., Rohe, L., 2024. Microbial nitrogen transformations tracked by natural abundance isotope studies and microbiological methods: a review. Science of the Total Environment 926, 172073.

Decock, C., Six, J., 2013. How reliable is the intramolecular distribution of ^{15}N in N_2O to source partition N_2O emitted from soil? Soil Biology and Biochemistry 65, 114–127.

Denk, T.R.A., Mohn, J., Decock, C., Lewicka-Szczebak, D., Harris, E., Butterbach-Bahl, K., Kiese, R., Wolf, B., 2017. The nitrogen cycle: a review of isotope effects and isotope modeling approaches. Soil Biology and Biochemistry 105, 121–137.

Friedl, J., Cardenas, L.M., Clough, T.J., Dannenmann, M., Hu, C., Scheer, C., 2020. Measuring denitrification and the N_2O:(N_2O + N_2) emission ratio from terrestrial soils. Current Opinion in Environmental Sustainability 47, 61–71.

Gallarotti, N., Barthel, M., Verhoeven, E., Pereira, E.I.P., Bauters, M., Baumgartner, S., Drake, T.W., Boeckx, P., Mohn, J., Longepierre, M., Mugula, J.K., Makelele, I.A., Ntaboba, L.C., Six, J., 2021. In-depth analysis of N_2O fluxes in tropical forest soils of the Congo Basin combining isotope and functional gene analysis. ISME Journal 15, 3357–3374.

Gao, D., Hou, L., Liu, M., Li, X., Zheng, Y., Yin, G., Wu, D., Yang, Y., Han, P., Liang, X., Dong, H., 2020. Mechanisms responsible for N_2O emissions from intertidal soils of the Yangtze Estuary. Science of the Total Environment 716, 137073.

Gao, N., Zhang, F., Bo, Q., Tang, A., Gao, J., Wei, X., Yue, S., Shen, Y., Li, S., 2023. Microbial and isotopomer analysis of N_2O production pathways in a calcareous film-mulched farmland. Biology and Fertility of Soils 59, 407–422.

Gilbert, M., Nicolas, G., Cinardi, G., Van Boeckel, T.P., Vanwambeke, S.O., Wint, G.R.W., Robinson, T.P., 2018. Global distribution data for cattle, buffaloes, horses, sheep, goats, pigs, chickens and ducks in 2010. Scientific Data 5, 180227.

Goldberg, S.D., Knorr, K.H., Gebauer, G., 2008. N_2O concentration and isotope signature along profiles provide deeper insight into the fate of N_2O in soils. Isotopes in Environmental and Health Studies 44, 377–391.

Gruber, W., Magyar, P.M., Mitrovic, I., Zeyer, K., Vogel, M., von Kanel, L., Biolley, L., Werner, R.A., Morgenroth, E., Lehmann, M.F., Braun, D., Joss, A., Mohn, J., 2022. Tracing N_2O formation in full-scale wastewater treatment with natural abundance isotopes indicates control by organic substrate and process settings. Water Research X 15, 100130.

Guo, S., Wu, J., Han, Z., Li, Z., Xu, P., Liu, S., Wang, J., Zou, J., 2022. The legacy effect of biochar application on soil nitrous oxide emissions. Global Change Biology Bioenergy 15, 478–493.

Harris, E., Diaz-Pines, E., Stoll, E., Schloter, M., Schulz, S., Duffner, C., Li, K., Moore, K.L., Ingrisch, J., Reinthaler, D., Zechmeister-Boltenstern, S., Glatzel, S., Brueggemann, N., Bahn, M., 2021. Denitrifying pathways dominate nitrous oxide emissions from managed grassland during drought and rewetting. Science Advances 7, eabb7118.

Harris, E.J., Fischer, P., Lewicki, M.P., Lewicka-Szczebak, D., Harris, S.J., Perez-Cruz, F., 2023. Technical note: TimeFRAME - a bayesian mixing model to unravel isotopic data and quantify trace gas production and consumption pathways for timeseries data. EGUsphere 2836.

Henry, S., Bru, D., Stres, B., Hallet, S., Philippot, L., 2006. Quantitative detection of the *nosZ* gene, encoding nitrous oxide reductase, and comparison of the abundances of *16S* rRNA, *narG, nirK*, and *nosZ* genes in soils. Applied and Environmental Microbiology 72, 5181–5189.

Ho, L., Barthel, M., Panique-Casso, D., Vermeulen, K., Bruneel, S., Liu, X., Bode, S., Six, J., Boeckx, P., Goethals, P., 2023. Impact of salinity gradient, water pollution and land use types on greenhouse gas emissions from an urbanized estuary. Environment and Pollution 336, 122500.

Hu, H.W., Chen, D., He, J.Z., 2015. Microbial regulation of terrestrial nitrous oxide formation: understanding the biological pathways for prediction of emission rates. FEMS Microbiology Reviews 39, 729–749.

Hu, H.W., Trivedi, P., He, J.Z., Singh, B.K., 2017. Microbial nitrous oxide emissions in dryland ecosystems: mechanisms, microbiome and mitigation. Environmental Microbiology 19, 4808–4828.

Ibraim, E., Denk, T., Wolf, B., Barthel, M., Gasche, R., Wanek, W., Zhang, S., Kiese, R., Butterbach-Bahl, K., Eggleston, S., Emmenegger, L., Six, J., Mohn, J., 2020. Denitrification is the main nitrous oxide source process in grassland soils according to quasi-continuous isotopocule analysis and biogeochemical modeling. Global Biogeochemical Cycles 34, e2019GB006505.

Ibraim, E., Wolf, B., Harris, E., Gasche, R., Wei, J., Yu, L., Kiese, R., Eggleston, S., Butterbach-Bahl, K., Zeeman, M., Tuzson, B., Emmenegger, L., Six, J., Henne, S., Mohn, J., 2019. Attribution of N_2O sources in a grassland soil with laser spectroscopy based isotopocule analysis. Biogeosciences 16, 3247–3266.

Kandeler, E., Deiglmayr, K., Tscherko, D., Bru, D., Philippot, L., 2006. Abundance of *narG, nirS, nirK*, and *nosZ* genes of denitrifying bacteria during primary successions of a glacier foreland. Applied and Environmental Microbiology 72, 5957–5962.

Kool, D.M., Dolfing, J., Wrage, N., Van Groenigen, J.W., 2011. Nitrifier denitrification as a distinct and significant source of nitrous oxide from soil. Soil Biology and Biochemistry 43, 174–178.

Krüger, M., Frenzel, P., Conrad, R., 2001. Microbial processes influencing methane emission from rice fields. Global Change Biology 7, 49–63.

Kuang, W., Gao, X., Tenuta, M., Gui, D., Zeng, F., 2019. Relationship between soil profile accumulation and surface emission of N_2O: effects of soil moisture and fertilizer nitrogen. Biology and Fertility of Soils 55, 97–107.

Leitner, S., Homyak, P.M., Blankinship, J.C., Eberwein, J., Jenerette, G.D., Zechmeister-Boltenstern, S., Schimel, J.P., 2017. Linking NO and N_2O emission pulses with the mobilization of mineral and organic N upon rewetting dry soils. Soil Biology and Biochemistry 115, 461–466.

Leitner, S.M., Carbonell, V., Mhindu, R.L., Zhu, Y., Mutuo, P., Butterbach-Bahl, K., Merbold, L., 2024. Greenhouse gas emissions from cattle enclosures in semi-arid sub-Saharan Africa: the case of a rangeland in South-Central Kenya. Agriculture, Ecosystems & Environment 367, 108980.

Lewicka-Szczebak, D., Augustin, J., Giesemann, A., Well, R., 2017. Quantifying N_2O reduction to N_2 based on N_2O isotopocules – validation with independent methods (helium incubation and ^{15}N gas flux method). Biogeosciences 14, 711–732.

Lewicki, M.P., Lewicka-Szczebak, D., Skrzypek, G., 2022. FRAME-Monte Carlo model for evaluation of the stable isotope mixing and fractionation. PLoS One 17, e0277204.

Li, X., Tang, C., Cao, Y., Li, X., 2021a. Isotope and isotopomer ratios of dissolved N_2O as indicators of nitrogen apportionment and transformation in shallow groundwater in Dongguan, southern China. Journal of Hydrology 600, 126514.

Li, Y., Zheng, Q., Yang, R., Zhuang, S., Lin, W., Li, Y., 2021b. Evaluating microbial role in reducing N_2O emission by dual isotopocule mapping following substitution of inorganic fertilizer for organic fertilizer. Journal of Cleaner Production 326, 129442.

Liang, X., Wang, B., Gao, D., Han, P., Zheng, Y., Yin, G., Dong, H., Tang, Y., Hou, L., 2022. Nitrification regulates the spatiotemporal variability of N_2O emissions in a eutrophic lake. Environmental Science and Technology 56, 17430–17442.

Marshall, F., Reid, R.E.B., Goldstein, S., Storozum, M., Wreschnig, A., Hu, L., Kiura, P., Shahack-Gross, R., Ambrose, S.H., 2018. Ancient herders enriched and restructured African grasslands. Nature 561, 387–390.

Muchiru, A.N., Western, D., Reid, R.S., 2009. The impact of abandoned pastoral settlements on plant and nutrient succession in an African savanna ecosystem. Journal of Arid Environments 73, 322–331.

Muchiru, A.N., Western, D.J., Reid, R.S., 2008. The role of abandoned pastoral settlements in the dynamics of African large herbivore communities. Journal of Arid Environments 72, 940–952.

Nishina, K., Melling, L., Toyoda, S., Itoh, M., Terajima, K., Waili, J.W.B., Wong, G.X., Kiew, F., Aeries, E.B., Hirata, R., Takahashi, Y., Onodera, T., 2023. Dissolved N_2O concentrations in oil palm plantation drainage in a peat swamp of Malaysia. Science of the Total Environment 872, 162062.

Pandey, C.B., Kumar, U., Kaviraj, M., Minick, K.J., Mishra, A.K., Singh, J.S., 2020. DNRA: a short-circuit in biological N-cycling to conserve nitrogen in terrestrial ecosystems. Science of the Total Environment 738, 139710.

Pelster, D.E., Gisore, B., Goopy, J., Korir, D., Koske, J.K., Rufino, M.C., Butterbach-Bahl, K., 2016. Methane and nitrous oxide emissions from cattle excreta on an East African grassland. Journal of Environmental Quality 45, 1531–1539.

Ravishankara, A.R., Daniel, J.S., Portmann, R.W., 2009. Nitrous oxide (N_2O): the dominant ozone-depleting substance emitted in the 21st century. Science 326, 123–125.

Sanford, R.A., Wagner, D.D., Wu, Q., Chee-Sanford, J.C., Thomas, S.H., Cruz-García, C., Rodríguez, G., Massol-Deyá, A., Krishnani, K.K., Ritalahti, K.M., Nissen, S., Konstantinidis, K.T., Löffler, F.E., 2012. Unexpected nondenitrifier nitrous oxide reductase gene diversity and abundance in soils. Proceedings of the National Academy of Sciences 109, 19709–19714.

Schauss, K., Focks, A., Leininger, S., Kotzerke, A., Heuer, H., Thiele-Bruhn, S., Sharma, S., Wilke, B.M., Matthies, M., Smalla, K., Munch, J.C., Amelung, W., Kaupenjohann, M., Schloter, M., Schleper, C., 2009. Dynamics and functional relevance of ammonia-oxidizing archaea in two agricultural soils. Environmental Microbiology 11, 446–456.

Scholes, M.C., Martin, R., Scholes, R.J., Parsons, D., Winstead, E., 1997. NO and N_2O emissions from savanna soils following the first simulated rains of the season. Nutrient Cycling in Agroecosystems 48, 115–122.

Silver, W.L., Herman, D.J., Firestone, M.K., 2001. Dissimilatory nitrate reduction to ammonium in upland tropical forest soils. Ecology 82, 2410–2416.

Su, X., Wen, T., Wang, Y., Xu, J., Cui, L., Zhang, J., Xue, X., Ding, K., Tang, Y., Zhu, Y.G., 2021. Stimulation of N_2O emission via bacterial denitrification driven by acidification in estuarine sediments. Global Change Biology 27, 5564–5579.

Su, X., Yang, L., Yang, K., Tang, Y., Wen, T., Wang, Y., Rillig, M.C., Rohe, L., Pan, J., Li, H., Zhu, Y.G., 2022. Estuarine plastisphere as an overlooked source of N_2O production. Nature Communications 13, 3884.

Syakila, A., Kroeze, C., 2011. The global nitrous oxide budget revisited. Greenhouse Gas Measurement and Management 1, 17–26.

Tian, H., Lu, C., Ciais, P., Michalak, A.M., Canadell, J.G., Saikawa, E., Huntzinger, D.N., Gurney, K.R., Sitch, S., Zhang, B., Yang, J., Bousquet, P., Bruhwiler, L., Chen, G., Dlugokencky, E., Friedlingstein, P., Melillo, J., Pan, S., Poulter, B., Prinn, R., Saunois, M., Schwalm, C.R., Wofsy, S.C., 2016. The terrestrial biosphere as a net source of greenhouse gases to the atmosphere. Nature 531, 225–228.

Tian, H., Xu, R., Canadell, J.G., Thompson, R.L., Winiwarter, W., Suntharalingam, P., Davidson, E.A., Ciais, P., Jackson, R.B., Janssens-Maenhout, G., Prather, M.J., Regnier, P., Pan, N., Pan, S., Peters, G.P., Shi, H., Tubiello, F.N., Zaehle, S., Zhou, F., Arneth, A., Battaglia, G., Berthet, S., Bopp, L., Bouwman, A.F., Buitenhuis, E.T., Chang, J., Chipperfield, M.P., Dangal, S.R.S., Dlugokencky, E., Elkins, J.W., Eyre, B. D., Fu, B., Hall, B., Ito, A., Joos, F., Krummel, P.B., Landolfi, A., Laruelle, G.G., Lauerwald, R., Li, W., Lienert, S., Maavara, T., MacLeod, M., Millet, D.B., Olin, S., Patra, P.K., Prinn, R.G., Raymond, P.A., Ruiz, D.J., van der Werf, G.R., Vuichard, N., Wang, J., Weiss, R.F., Wells, K.C., Wilson, C., Yang, J., Yao, Y., 2020. A comprehensive quantification of global nitrous oxide sources and sinks. Nature 586, 248–256.

Tiedje, J.M., 1998. Ecology of denitrification and dissimilatory nitrate reduction to ammonium. Biology of Anaerobic Microorganisms 717, 179–244.

Tischer, J., Zopfi, J., Frey, C., Magyar, P.M., Brand, A., Oswald, K., Jegge, C., Frame, C. H., Miracle, M.R., Sòria-Perpinyà, X., Vicente, E., Lehmann, M.F., 2022. Isotopic signatures of biotic and abiotic N_2O production and consumption in the water column of meromictic, ferruginous Lake La Cruz (Spain). Limnology & Oceanography 67, 1760–1775.

Toyoda, S., Yano, M., Nishimura, S.-i., Akiyama, H., Hayakawa, A., Koba, K., Sudo, S., Yagi, K., Makabe, A., Tobari, Y., Ogawa, N.O., Ohkouchi, N., Yamada, K., Yoshida, N., 2011. Characterization and production and consumption processes of N_2O emitted from temperate agricultural soils determined via isotopomer ratio analysis. Global Biogeochemical Cycles 25, 1–17.

Tubiello, F.N., Salvatore, M., Cóndor Golec, R.D., Ferrara, A., Rossi, S., Biancalani, R., Federici, S., Jacobs, H., Flammini, A., 2014. Agriculture, forestry and other land use emissions by sources and removals by sinks 1990–2011 analysis. FAO Statistics Division Working Paper 4, 375–376.

Verhoeven, E., Barthel, M., Yu, L., Celi, L., Said-Pullicino, D., Sleutel, S., Lewicka-Szczebak, D., Six, J., Decock, C., 2019. Early season N_2O emissions under variable water management in rice systems: source-partitioning emissions using isotope ratios along a depth profile. Biogeosciences 16, 383–408.

Wachiye, S., Merbold, L., Vesala, T., Rinne, J., Räsänen, M., Leitner, S., Pellikka, P., 2020. Soil greenhouse gas emissions under different land-use types in savanna ecosystems of Kenya. Biogeosciences 17, 2149–2167.

Wang, Y., Guo, J., Vogt, R.D., Mulder, J., Wang, J., Zhang, X., 2018. Soil pH as the chief modifier for regional nitrous oxide emissions: new evidence and implications for global estimates and mitigation. Global Change Biology 24, e617–e626.

Wei, H., Song, X., Liu, Y., Wang, R., Zheng, X., Butterbach-Bahl, K., Venterea, R.T., Wu, D., Ju, X., 2023. In situ ^{15}N-N_2O site preference and O_2 concentration dynamics disclose the complexity of N_2O production processes in agricultural soil. Global Change Biology 29, 4910–4923.

Well, R., Maier, M., Lewicka-Szczebak, D., Köster, J.-R., Ruoss, N., 2019. Underestimation of denitrification rates from field application of the ^{15}N gas flux method and its correction by gas diffusion modelling. Biogeosciences 16, 2233–2246.

WMO, 2021. The state of greenhouse gases in the atmosphere based on global observations through 2020. WMO Greenhouse Gas Bulletin 17, 1–10.

Wolf, B., Merbold, L., Decock, C., Tuzson, B., Harris, E., Six, J., Emmenegger, L., Mohn, J., 2015. First on-line isotopic characterization of N_2O above intensively managed grassland. Biogeosciences 12, 2517–2531.

Wrage, N., Velthof, G.L., van Beusichem, M.L., O, O., 2001. Role of nitrifier denitrification in the production of nitrous oxide. Soil Biology and Biochemistry 33, 1723–1732.

Wu, D., Well, R., Cardenas, L.M., Fuss, R., Lewicka-Szczebak, D., Koster, J.R., Bruggemann, N., Bol, R., 2019. Quantifying N_2O reduction to N_2 during denitrification in soils via isotopic mapping approach: model evaluation and uncertainty analysis. Environmental Research 179, 108806.

Yu, L., Harris, E., Lewicka-Szczebak, D., Barthel, M., Blomberg, M.R.A., Harris, S.J., Johnson, M.S., Lehmann, M.F., Liisberg, J., Muller, C., Ostrom, N.E., Six, J., Toyoda, S., Yoshida, N., Mohn, J., 2020. What can we learn from N_2O isotope data? - analytics, processes and modelling. Rapid Communications in Mass Spectrometry 34, e8858.

Zhang, Y., Zhang, F., Abalos, D., Luo, Y., Hui, D., Hungate, B.A., Garcia-Palacios, P., Kuzyakov, Y., Olesen, J.E., Jorgensen, U., Chen, J., 2022. Stimulation of ammonia oxidizer and denitrifier abundances by nitrogen loading: poor predictability for increased soil N_2O emission. Global Change Biology 28, 2158–2168.

Zhu, Y., Butterbach-Bahl, K., Merbold, L., Oduor, C.O., Gakige, J.K., Mwangi, P., Leitner, S.M., 2024. Greenhouse gas emissions from sheep excreta deposited onto tropical pastures in Kenya. Agriculture, Ecosystems & Environment 359, 108724.